Synthesis, molecular properties and DFT studies of new phosphoramidates as potential urease inhibitors

ARTICLE *in* MEDICINAL CHEMISTRY RESEARCH · JUNE 2014

Impact Factor: 1.4 · DOI: 10.1007/s00044-014-1113-y

7 AUTHORS, INCLUDING:

Fabrício Marques de Oliveira
Universidade Federal de Viçosa (UFV)
10 PUBLICATIONS **24** CITATIONS
SEE PROFILE

Luiz Claudio De Almeida Barbosa
Federal University of Minas Gerais
355 PUBLICATIONS **2,123** CITATIONS
SEE PROFILE

Lívia Pereira Horta
Federal University of Minas Gerais
7 PUBLICATIONS **13** CITATIONS
SEE PROFILE

Luzia V Modolo
Federal University of Minas Gerais
55 PUBLICATIONS **1,098** CITATIONS
SEE PROFILE

Med Chem Res
DOI 10.1007/s00044-014-1113-y

MEDICINAL CHEMISTRY RESEARCH

ORIGINAL RESEARCH

Synthesis, molecular properties and DFT studies of new phosphoramidates as potential urease inhibitors

Fabricio M. Oliveira · Luiz C. A. Barbosa · Antônio J. Demuner · Célia R. A. Maltha · Silvana R. Pereira · Lívia P. Horta · Luzia V. Modolo

Received: 24 April 2014 / Accepted: 16 June 2014

Abstract In this work, new phosphoramidates were prepared and screened for their putative urease inhibitory activity. The importance of this class of compounds is related to the wide range of biological activities which they exhibit. Consequently, higher activity shown by phosphoramidates **3a**, **4b**, **5a**, **5b**, **5c**, and **9a** suggests that they could serve as lead substances for the development of novel synthetic compounds with enhanced inhibitory ureolitic activity. Their predicted ADMET properties are also in accordance with the general requirements for drug-like compounds. Structure–activity relationship analyses suggest that the presence of cyclohexylamine group is an important structural feature associated with enhanced activities. DFT calculations were performed to obtain the energy values of HOMO and LUMO, and dipole moment.

Keywords Urease inhibitors · Jack bean urease · Phosphoramidates · Canavalia ensiformis · DFT Studies

Electronic supplementary material The online version of this article (doi:10.1007/s00044-014-1113-y) contains supplementary material, which is available to authorized users.

F. M. Oliveira · L. C. A. Barbosa · A. J. Demuner · C. R. A. Maltha · S. R. Pereira
Departamento de Química, Universidade Federal de Viçosa, Av. PH Rolfs, Viçosa, MG 36570-000, Brazil

L. C. A. Barbosa (✉)
Departamento de Química, Universidade Federal de Minas Gerais, Av. Presidente Antônio Carlos 6627, Pampulha, Belo Horizonte, MG 31270-901, Brazil
e-mail: lcab@ufv.br; lcab@ufmg.br

L. P. Horta · L. V. Modolo
Departamento de Botânica, Universidade Federal de Minas Gerais, Av. Presidente Antônio Carlos 6627 – Pampulha, Belo Horizonte, MG 31270-901, Brazil

Introduction

Urease is a nickel-containing metalloenzyme that catalyzes hydrolysis of urea to ammonia and carbon dioxide and occur in a wide variety of organisms (Roberts *et al.*, 2012; Krajewska, 2009; Follmer, 2010). High concentration of ammonia arising from these reactions is responsible for the endurance of bacteria *Helicobacter pylori* to acidic pH of the stomach during colonization (Follmer, 2010; Amtul *et al.*, 2002). The enzymatic activity of urease plays an effective role in pathogenesis of urinary and gastrointestinal tracts, causing diseases such as gastritis, peptic ulcers, and gastric cancer (Follmer, 2010). Urease inhibitors play an important role in the treatment of infections caused by urease producing bacteria (Krajewska, 2009). Among such bacteria are *H. pylori*, a well-recognized pathogen that infects two-thirds of world population causing 2–4 % mortality among infected humans (Roberts *et al.*, 2012; Duckworth *et al.*, 2009). Currently, the treatment of infections caused by *H. pylori* has been accomplished through a combination of drugs due to the high level of antibiotic resistance exhibited by these bacteria (Roberts *et al.*, 2012). This highlights the need for the development of new antimicrobials to treat *H. pylori* infections, and one important line of research is to target the urease produced by this bacteria (Follmer, 2010; Amtul *et al.*, 2002; Li *et al.*, 2009).

Among the several classes of compounds known to inhibit ureases, the phosphoramidates represent the most active (Vassiliou *et al.*, 2008). This class of compounds have attracted much attention due to their wide range of biological activities such as insecticides (Paula *et al.*, 2008; Oliveira *et al.*, 2012a), anti-HCV (McGuigan *et al.*, 2009), anti-HIV (Derudas *et al.*, 2009; Mehellou *et al.*, 2009), antiviral (Harris *et al.*, 2001; Derudas *et al.*, 2010),

Published online: 28 June 2014

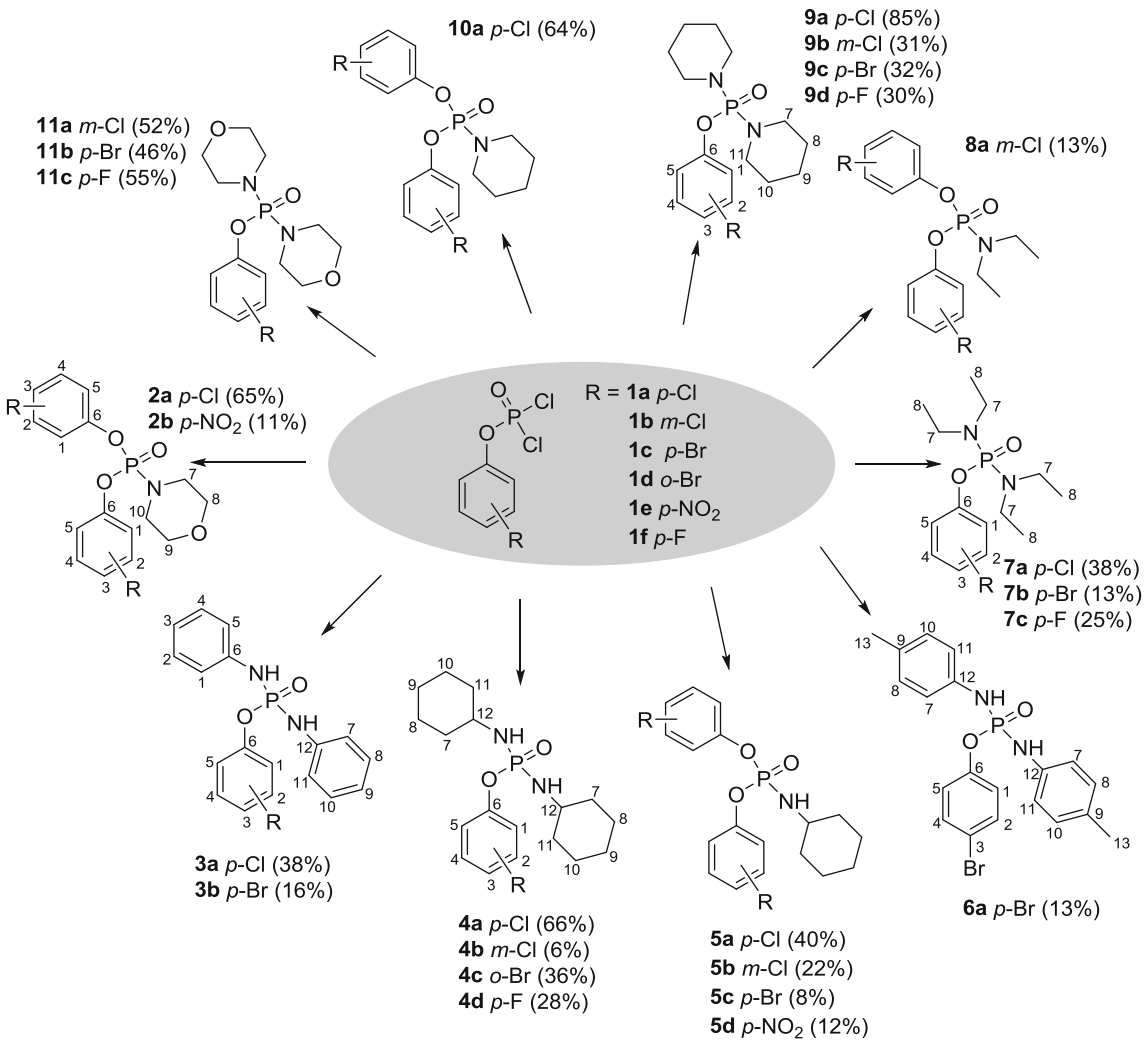

Scheme 1 Structural formulas of the phosphoramidates synthesized. In general, the conversion of **1a–f** to compounds **2–11** was achieved by reaction with different amines

inhibitor of reverse transcriptase (Borrello *et al.*, 2009), antimalarial (Mara *et al.*, 2011), and inhibitor of hepatitis C virus (Donghi *et al.*, 2009).

Thus, in the present work, new phosphoramidates were prepared and screened for inhibitory activity against urease from *Jack bean* using thiourea (TU) and hydroxyurea (HU) as reference urease inhibitors. Urease activity was determined by measuring the ammonia production using the indophenol method (Weatherburn, 1967). In addition, the map of the electrostatic potential (MEP) and the value of the frontier orbitals HOMO and LUMO and the dipole moment for optimized geometries from DFT calculations were investigated, as these features may be related to the interaction of the molecules with their target sites. In silico physicochemical properties of the evaluated compounds were determined, and the results are also discussed.

The target compounds were synthesized by employing a short synthetic sequence (Scheme 1) according to a procedure adapted from the literature (Uckun *et al.*, 2005). In the initial step, a mixture of substituted phenols, phosphoryl chloride, and triethylamine in dry diethyl ether was stirred for 18 h at room temperature resulting in the intermediates **1a–f**, which were used without purification as shown in Scheme 1.

The intermediates **1a–f** were treated with different amines (two equivalents) and triethylamine (two equivalents) in anhydrous dichloromethane, and the mixture was maintained under magnetic stirring for 18 h. In sequence, the precipitate formed was removed by vacuum filtration on a sintered glass funnel and the precipitate washed with anhydrous dichloromethane to afford the required products **2–11** (Scheme 1). Several attempts to optimize this reaction were carried out, varying the amount of solvent,

temperature, reaction time, etc. However, in some cases, only a small amount of the required product was formed, and in general, the yields of the required compounds varied from 6 to 91 % after purification on a silica gel column. The formation of bisarylphosphonates compounds (**5a–d, 8a, 10a**) may have been favored since the intermediates **1a–f** were used in the next step without further purification. Moreover, these intermediates can be degraded to the respective phenols. Spectroscopic data (IR, ^{1}H NMR, and ^{13}C NMR) of all the synthesized compounds were in full agreement with the proposed structures (see "Experimental" section).

The effect of each compound was assessed by comparing the inhibitory characteristic of the phosphoramidates with that of TU and HU, the standard compounds which belong to the urease inhibitor group of molecules. The inhibition of ureolitic activity of tested compounds varied from 4 to 83 %. Compounds **4c**, **4d**, **5d**, **9c**, **9d**, **11b,** and **c**, however, were found to be positive allosteric effectors on urease as they stimulated urea hydrolysis assisted by this enzyme (Table 1).

The phosphoramidates **11a** and **2b** stimulated urease activity only in experiments carried out with urea concentrations as high as 20 mM. The phosphoramidates **3a**, **4b**, **5a**, **b**, **c,** and **9a** were found to be the most promising urease inhibitors (Table 1). Thus, these compounds were further investigated, and their IC_{50} (concentration necessary to inhibit urease by 50 %) were determined.

Table 2 shows that compound **5c** was approximately as potent as HU and four times more potent than the reference urease inhibitor TU, under the test experimental conditions. The second best urease inhibitor was the compound **5b** followed by **5a**, **9a**, **4b**, and **3a**. From the results presented in Table 2, it can be observed that with exception of **3a** all the other compounds were more potent than TU.

Since the phosphoramidates inhibited the urease activity at different extents, a cluster analysis employing data obtained at 10–20 mM was obtained in order to facilitate the grouping of these compounds and a comparison with standard urease inhibitors HU and TU (Fig. 1).

As can be observed in Fig. 1, four main groups of compounds were formed: G1 and G2 include compounds that are poor urease inhibitors, including the reference TU; and G3 and G4 include compounds that are better active urease inhibitors compared with the standard (HU). The inhibitory ureolitic activity of compounds **5a** and **c** was comparable to that of the HU, **5c** being the most active one. Among the three most active phophoramidates (shown in G3 and G4), all of them bear the cyclohexylamine group, which highlights the importance of this unit for biological activity. The phenoxy group seems to not contribute for the inhibitory ureolitic activity of the synthesized phosphoramidates as such group is present in all compounds, including those that function as positive allosteric effectors. Compounds prepared from *p*-bromophenol (**1c**, **3b**, **5c**, **6a**, **7b**, **9c**, and **11b**), *p*-chlorophenol (**1a**, **2a**, **3a**, **4a**, **5a**, **7a**, **9a,**

Table 1 In vitro urease inhibitory activities of phosphoramidates **2–11**

Compound	Urea (mM)	
	10.0	20.0
2a	36.53 ± 0.81	29.07 ± 3.83
2b	5.20 ± 1.73	−4.05 ± 5.95
3a	29.00 ± 7.30	50.74 ± 3.44
3b	50.25 ± 1.61	29.45 ± 1.93
4a	33.77 ± 2.68	30.95 ± 1.56
4b	36.00 ± 4.80	83.60 ± 0.36
4c	−31.97 ± 4.68	−11.43 ± 14.43
4d	−13.47 ± 2.13	−5.28 ± 2.60
5a	69.42 ± 4.00	79.45 ± 3.03
5b	46.00 ± 11.00	50.54 ± 7.38
5c	72.05 ± 6.15	74.04 ± 6.96
5d	−39.39 ± 0.56	−11.34 ± 0.45
6a	39.49 ± 10.77	52.37 ± 4.14
7a	23.32 ± 0.30	10.22 ± 2.74
7b	16.44 ± 5.13	23.75 ± 1.84
7c	5.15 ± 5.37	17.00 ± 6.41
8a	15.61 ± 5.34	3.97 ± 10.94
9a	62.05 ± 2.27	47.00 ± 0.33
9b	17.00 ± 4.56	13.29 ± 19.61
9c	−25.37 ± 0.57	−8.95 ± 3.56
9d	−9.29 ± 0.46	−5.25 ± 0.01
10a	30.24 ± 1.15	33.65 ± 0.44
11a	15.69 ± 0.23	−3.89 ± 1.48
11b	−47.70 ± 5.56	−20.55 ± 1.52
11c	−45.76 ± 0.78	−16.64 ± 2.16
Hydroxyurea (HU)	80.02 ± 6.03	71.18 ± 6.07
Thiourea(TU)	22.62 ± 13.78	20.33 ± 11.32

Values are the mean ± SD from three experiments ($n = 3$). Hydroxyurea and thiourea were used as reference of urease inhibitors

Table 2 Concentration of promising phosphoramidates necessary to inhibit urease by 50 % (IC_{50})

Compound	IC_{50} (mM)
3a	2.77
4b	2.28
5a	1.16
5b	0.98
5c	0.69
9a	1.44
Hydroxyurea (HU)	0.61
Thiourea (TU)	2.72

Reactions were carried out in the presence of urea 10 mM

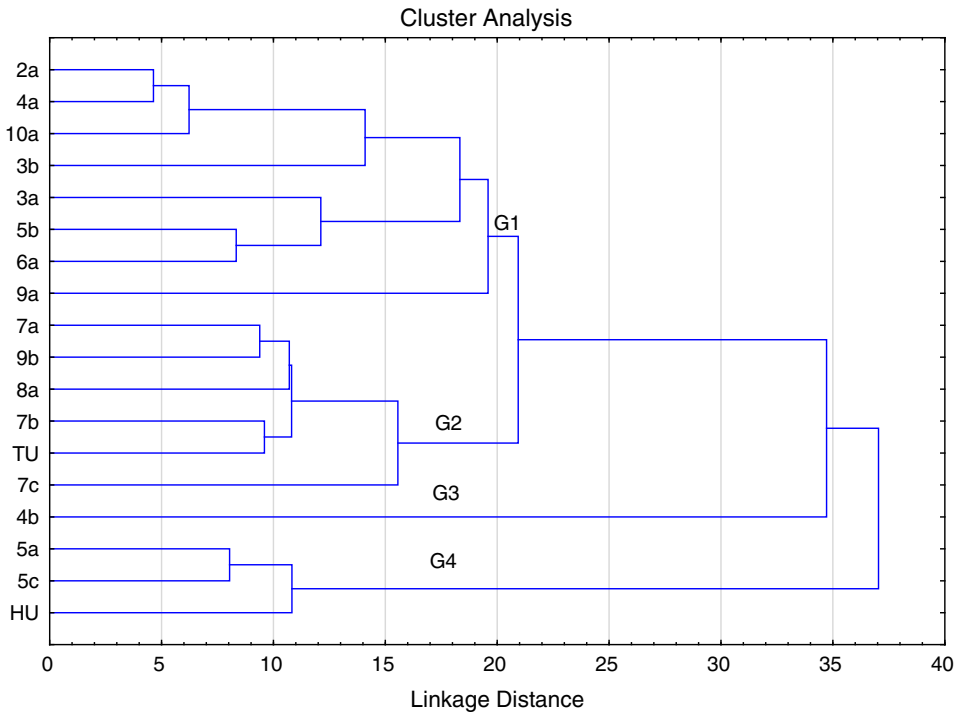

Fig. 1 Cluster analysis for phosphoramidates. (*TU* thiourea and *HU* hydroxyurea)

and **10a**), or *m*-chlorophenol (**1b**, **4b**, **5b**, **8a**, **9b**, and **11a**) were among the most active, while compounds derived from *p*-nitrophenol (**1e**, **2b**, and **5b**), *o*-bromophenol (**1d** and **4c**), or *p*-fluorophenol (**1f**, **4d**, **7c**, **9d**, and **11c**) were less active. However, it is important to highlight that the presence of phenol groups per se is not the main feature associated with biological activity since some compounds containing *p*-chlorophenol (**2a**, **3a**, **4a**, and **10a**) and *p*-bromophenol (**3b** and **6a**) were poorly active.

A computational study was carried out to predict their physicochemical properties, since it is related to the absorption, distribution, metabolism, excretion, and toxicity (ADMET) properties (Mangal *et al.*, 2013). Screening was conducted to evaluate the characteristics of the candidate drugs based on Lipinski's Rule of Five (Lipinski *et al.*, 1997) and other related criteria added by Veber and co-workers (Veber *et al.*, 2002). The molecular attributes analyzed included the calculated octan-1-ol/water partition coefficient ($c\text{Log}P \leq 5$); number of hydrogen bond donors (HBD ≤ 5); number of hydrogen bond acceptors (HBA ≤ 10); molecular weight (MW ≤ 500); number of rotatable bonds (nRotb < 10); and topological polar surface area (TPSA < 140 Å^2). Values in parentheses represent the ideal values according to Lipinski (Lipinski *et al.*, 1997) and Veber (Veber *et al.*, 2002). Physicochemical parameters (Tables 3, 4) were calculated using osiris property explorer (Tetko, 2005) and Molinspiration (http://www.molinspiration.com/cgi-bin/properties), good free computational tools which help predict pharmacokinetic properties of candidate drugs used by several research groups (Alafeefy *et al.*, 2012; Oliveira *et al.*, 2012b; Teixeira *et al.*, 2013).

Normally, the drugs interacting with enzymes inside the body have Log*P* values between 2 and 5 (Tambunan *et al.*, 2011). In this respect, most of the 25 compounds present Log*P* values within this range, the exceptions being compounds **5a**, **b**, **c**, and **6a** (Tables 2, 3). Interestingly to note is that despite the high LogP values, compounds **5a**, **b**, **c** are among the most actives.

Analysis of theoretical toxicity risks revealed that all compounds examined might not be tumorigenic or irritating (Table 3). However, five compounds might have mutagenic effect (**3b**, **5c**, **6a**, **9c**, and **11b**), and two could possibly have some effect on mammalian reproduction (**4d** and **2b**) (Table 3). With regard to solubility in water of organic molecules (log *S*), only compounds **5c** ($\log S = -6.57$) and **6a** ($\log S = -7.19$) present solubility values outside the limits (−6.5 to 0.5) (Maalej *et al.*, 2011). The negative values of the drug-likeness calculations, between −28.83 and −11.68 (Table 3), indicate that compounds of the series **2**–**11** do not contain fragments that are frequently present in commercial drugs (Lipinski *et al.*, 2001; Proudfoot, 2002).

Compound **2b** is the one with the highest HBA number (equal to 9), close to the limit of 10 predicted by Lipinsky's rule. On the other hand, some compounds (**4a**, **3a**, **4b**, **c**, **d**, **3b**, and **6a**) show values of HBD = 2, while HU presents HBD = 4. From the data presented so far for compounds

Table 3 Predicted drug-likeness properties and toxicity risks of compounds calculated by Osiris package

Comp.				Toxicity risks[a]					
	*c*Log*P*	Log*S*	MW	M	T	I	R	Drug-likeness	Drug-score
2a	3.61	−4.45	388	−	−	−	−	−15.79	0.33
2b	0.3	−1.87	357	−	−	−	±	−23.46	0.36
3a	4.37	−6.40	358	−	−	−	−	−11.68	0.23
3b	4.46	−6.5	403	±	−	−	−	−15.17	0.17
4a	4.62	−5.99	370	−	−	−	−	−16.24	0.23
4b	4.62	−5.99	370	−	−	−	−	−17.52	0.23
4c	4.70	−6.09	415	−	−	−	−	−21.01	0.21
4e	4.07	−5.57	354	−	−	−	−	−18.55	0.27
5a	5.4	−6.37	400	−	−	−	−	−21.03	0.19
5b	5.4	−6.37	400	−	−	−	−	−22.31	0.19
5c	5.57	−6.57	489	±	−	−	−	−24.22	0.12
5d	4.07	−5.57	354	−	−	−	−	−18.55	0.27
6a	5.09	−7.19	431	±	−	−	−	−16.61	0.14
7a	3.77	−3.21	318	−	−	−	−	−15.72	0.39
7b	3.21	−2.79	363	−	−	−	−	−18.05	0.42
7c	3.21	−2.79	302	−	−	−	−	−18.05	0.42
8a	4.97	−4.98	374	−	−	−	−	−21.84	0.26
9a	3.46	−3.92	342	−	−	−	−	−11.95	0.37
9b	3.46	−3.92	342	−	−	−	−	−13.09	0.37
9c	3.54	−4.02	387	±	−	−	−	−15.0	0.28
9d	2.9	−3.50	326	−	−	−	−	−14.14	0.41
10a	4.82	−5.84	386	−	−	−	−	−16.74	0.25
11a	1.04	−2.15	346	−	−	−	−	−12.13	0.45
11b	1.12	−2.24	391	±	−	−	−	−14.04	0.34
11c	0.49	−1.72	330	−	−	−	−	−13.19	0.46
Hydroxyurea	−1.45	−1.00	76.0	−	−	−	−	−0.19	0.09
Thiourea	−0.95	−0.88	76.0	−	−	−	−	−2.21	0.54

*c*Log*P* calculated lipophilicity, *logS* logarithm of aqueous solubility measured in M, *MW* molecular weight, *M* mutagenic effect, *T* tumorigenic effect, *I* irritating effect, *R* reproductive effect

[a] Ranked according to: (−) no bad effect, (±) medium bad effect, (+) bad effect

Table 4 Drug-likeness calculations of compounds using Molinspiration Cheminformatics software

Comp.	TPSA	HBD	HBA	Lipinski's violations	Volume	nRotB	%ABS[a]
2a	48.01	0	5	0	306.974	5	92.44
2b	97.07	0	9	0	300.977	5	75.51
3a	50.36	2	4	0	302.533	6	91.63
3b	50.36	2	4	1	306.882	6	91.63
4a	50.35	2	4	1	339.705	6	91.63
4b	50.36	2	4	1	339.705	6	91.63
4c	50.36	2	4	1	344.055	6	91.63
4e	50.36	2	4	0	331.101	6	91.63
5a	47.57	1	4	1	331.237	6	92.59
5b	47.57	1	4	1	331.237	6	92.59
5c	47.57	1	4	1	339.936	6	92.59
5d	50.36	2	4	0	331.101	6	91.63
6a	50.36	2	4	1	340.004	6	91.63
7a	32.78	0	4	0	293.93	8	97.69
7b	32.78	0	4	0	298.279	8	97.69
7c	32.781	0	4	0	285.325	8	97.69
8a	38.78	0	4	1	308.349	7	95.62
9a	32.78	0	4	0	306.813	4	97.69
9b	32.78	0	4	0	306.813	4	97.69
9c	32.78	0	4	0	311.162	4	97.69
9d	32.78	0	4	0	298.208	4	97.69
10a	38.77	0	4	1	314.791	5	95.62
11a	51.25	0	6	0	291.179	4	91.32
11b	51.25	0	6	0	295.528	4	91.32
11c	51.249	0	6	0	282.574	4	91.32
HU	75.349	4	4	0	63.327	0	83.00
TU	52.046	2	4	0	63.074	0	91.04

HBD number of hydrogen bond donor, *HBA* number of hydrogen bond acceptor, *TPSA* total polar surface area, *HU* hydroxyurea, *TU* thiourea

[a] %ABS = 109 − 0.345 × TPSA (Ertl *et al.*, 2000)

of the series **2**–**11**, the parameters described in Lipinski's rules are within the limit set by such rules. Among the compounds studied, eleven of them have one rule violation, which is within the limits established (two) (Lipinski *et al.*, 2001). Only compounds **4d** (TPSA = 96.18) and **2b** (TPSA = 97.07) (Table 4) are expected to exhibit moderate bioavailability, based on the acceptable range ($61 \leq$ TPSA ≤ 140), while for others, it is expected a good bioavailability. TPSA was used to calculate the percentage of absorption (%ABS) as reported (Ertl *et al.*, 2000). From all these parameters, it can be observed that all the title compounds exhibited a great %ABS ranging from 75.51 to 97.69 %. In general, the compounds in this series possess a high nRotb (4–8) and, therefore, exhibit large conformational flexibility, while the standard's compounds presented nRotB = 0 (Table 4).

One factor closely related to the affinity of a receptor is the molecular volume. This parameter does not seem to have a direct relationship with the biological activity, since the compound used as a positive control (HU) showed small molecular volume (63 A^3) compared to compound **5c** (339.936 A^3).

In an attempt to find some correlation between electronic properties and biological activity (Correa-Basurto *et al.*, 2007; Arantes *et al.*, 2011), the HOMOs and LUMOs of the compounds were examined. The calculated energies gaps are also listed in Table 5. The computational

Table 5 Descriptors quantum chemical for compounds of series **2**–**11** and references

Comp.	HOMO	LUMO	GAP[a]	Moment dipole
2a	−6.61	−0.92	−5.69	4.14
2b	−6.35	−2.99	−3.36	8.35
3a	−6.19	−0.88	−5.32	5.78
3b	−6.01	−0.49	−5.52	5.77
4a	−6.50	−0.82	−5.68	6.55
4b	−6.56	−0.83	−5.72	8.62
4c	−6.36	−0.38	−5.98	3.44
4d	−6.58	−0.81	−5.77	6.63
5a	−6.67	−0.92	−5.75	6.44
5b	−6.86	−0.92	−5.94	5.55
5c	−6.49	−0.77	−5.72	6.43
5d	−7.05	−2.57	−4.48	5.96
6a	−5.98	−0.89	−5.10	6.27
7a	−6.32	−0.82	−5.51	7.25
7b	−6.09	−0.36	−5.72	6.72
7c	−6.04	−0.31	−5.74	6.28
8a	−6.77	−0.91	−5.86	3.39
9a	−6.31	−0.82	−5.49	7.03
9b	−6.29	−0.82	−5.47	4.89
9c	−6.21	−0.40	−5.82	6.99
9d	−6.39	−0.80	−5.59	6.51
10a	−6.66	−0.91	−5.74	6.28
11a	−6.28	−0.84	−5.44	2.45
11b	−6.26	−0.52	−5.73	4.51
11c	−6.23	−0.47	−5.76	4.07
Hydroxyurea	−7.60	−0.19	−7.41	5.00
Thiourea	−6.06	−0.33	−5.73	7.70

[a] GAP = HOMO–LUMO

calculations were performed using Spartan (Hehre and Ohlinger, 2010) and Gaussian (Frisch *et al*., 2009).

The IC_{50} values were converted to their related negative logarithmic state, which is $\log(1/IC_{50})$ and further used as dependent variable in developing the QSAR models. The descriptors used in the regression analysis are *c*Log*P*, HOMO energy, LUMO energy, GAP energy, moment dipole, and molecular volume (Tables 2, 3, 4).

Preliminary analysis was carried out in terms of a correlation analysis between $-\text{Log}IC_{50}$ and various molecular descriptors, and the results are presented in Table 6. This was done to remove the chances of intercorrelation among the molecular descriptors that may lead to false predicting models.

The values of the selected descriptors used in the regression analysis are presented in Tables 3, 4, 5. The models were built using the multiple linear regression (MLR) method as employed in the BuildQsar software (de Oliveira and Gaudio, 2001). The data depicted in Table 6 indicated poor correlation between urease activities with these descriptors (see graphs in the supplemental material). Thus, models using MLR method were obtained since it was not possible to validate using the leave-one-out (LOO) method (de Oliveira and Gaudio, 2001).

It appears that there is a correlation between the structure of compounds **HU**, **5b**, **5a**, **9a**, **TU**, and **4b** with the inhibitory activity of urease. Compounds **3a** and **5c** would be outliers in this linear regression ($-\text{Log}IC_{50} = -0.1333$ MD + 0.7885; $R^2 = 0.9823$). However, no plausible explanation to justify the removal of these compounds (**3a** and **5c**) can be proposed. Furthermore, the structures of the compounds used as positive control (HU and TU) differ significantly from the compounds synthesized in this work.

The highest and the lowest energy difference between the HOMO and LUMO (gap energies) were observed for compounds **4c** (−5.98 eV) and **2b** (−4.37 eV), respectively. However, it was not observed for these compounds under discussion a clear correlation of biological activity with the measures of nucleophilicity and electrophilicity (HOMO and LUMO energies, respectively). Figure 2 shows the distributions and energy levels of the frontier molecular orbital computed at the B3LYP/6-311 ++ G(2*d*,*p*) level for the most active compound (**5c**).

Experimental

Chemistry

All the chemicals were purchased from Sigma Aldrich (Milwaukee, WI, USA) and used without purification. The

Table 6 Correlation matrix for $-\text{Log}IC_{50}$ with molecular descriptors

	$-\text{Log}IC_{50}$	HOMO	LUMO	GAP	Moment dipole	Volume	*c*Log*P*
$-\text{Log}IC_{50}$	1.000						
HOMO	0.645	1.000					
LUMO	0.363	0.365	1.000				
GAP	0.649	0.927	0.686	1.000			
Moment dipole	0.589	0.578	0.105	0.503	1.000		
Volume	0.248	0.290	0.970	0.614	0.143	1.000	
*c*Log*P*	0.178	0.285	0.963	0.609	0.078	0.984	1.000

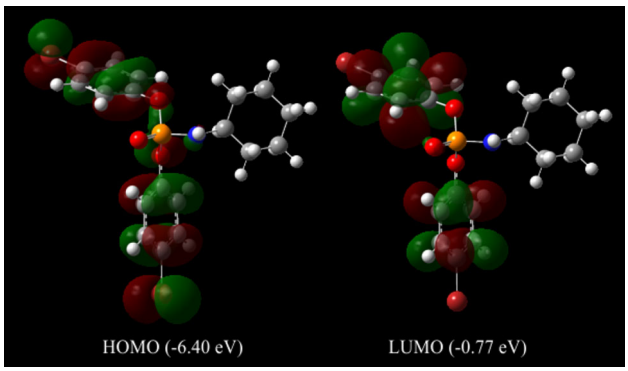

Fig. 2 Molecular orbital surfaces and energy levels given in parentheses for the HOMO and LUMO of the most active compound computed at B3LYP/6-311++G(2*d*,*p*) level in water

^{1}H- and ^{13}C-NMR spectra were recorded on a Varian Mercury 300 instrument (300 and 75 MHz respectively). Tetramethylsilane was used as internal standard ($\delta = 0$) and deuterated DMSO as solvent. IR spectra were obtained using a Perkin Elmer Paragon 1000 FTIR spectrophotometer, using potassium bromide (1 % v/v) disks, scanning from 600 to 4,000 cm^{-1}. HRMS data were recorded under ESI conditions on a micrOTOF-QII Bruker spectrometer. The melting points were determined using a MQAPF-301 melting point apparatus (Microquimica, Brazil) and were not corrected. Analytical thin layer chromatography analysis was conducted on aluminum-backed pre-coated silica gel plates. Flash column chromatography was performed using silica gel 60 (63–230 μm).

General method of preparation of phosphorodichloridate derivatives (**1a**–**1f**)

Phosphorus oxychloride (1.0 mL, 10.8 mmol) in dry diethyl ether (10.0 mL) was placed under a nitrogen atmosphere in a 50-mL round-bottom flask. The contents were cooled to 0 °C using an ice bath. A solution of substituted phenols (9.8 mmol) and triethylamine (1.5 mL, 10.8 mmol) in anhydrous diethyl ether (25 mL) was added dropwise while maintaining the temperature at 0 °C throughout the addition (ca: 1 h). After this period, the ice bath was removed, and the mixture was allowed to gradually warm up to room temperature and was stirred vigorously for 18 h. The precipitated triethylammonium salt was filtered through a sintered glass funnel under vacuum, and the precipitate was washed with additional anhydrous diethyl ether. The organic layers were combined, and the solvent was evaporated under vacuum using a rotary evaporator to yield crude phosphorodichloridate (**1a**–**f**) as viscous oil, which were used without further purification. The spectroscopic and spectrometric data of all compounds are consistent with predicted in the literature.

General method of preparation of phosphoramidates

Phosphorodichloridate derivatives (**1a**–**f**) (500 mg, 1.7 mmol) were placed into a round-bottom flask under nitrogen atmosphere. Using a dry syringe, anhydrous dichloromethane (10 mL) was added, and the mixture was cooled to 0 °C. A solution of different amines (6.9 mmol) in anhydrous dichloromethane (20 mL) was added dropwise with vigorous stirring over a period of 1 h. After completion of the addition, the reaction mixture was allowed to gradually warm to room temperature and stirred for 18–22 h until the reaction was complete as evidenced from TLC analyses. The crude products were concentrated in vacuum, anhydrous diethyl ether (15 mL) was added, and the precipitated triethylammonium hydrochloride salt was filtered. The precipitate was further washed with additional diethyl ether (2 × 15 mL). The combined ether extracts were combined and concentrated in a rotary evaporator under reduced pressure to afford the required compounds. The synthesis of compounds **2a**, **3a**, **4a**, **5a**, and **10a** is described in the literature (Krishnan *et al.*, 1985; Ruveda *et al.*, 1975; Roubinek *et al.*, 1980; Cramer *et al.*, 1961; Kašpárek and Mollin, 1980).

Spectral data

*Bis(4-chlorophenyl) morpholinophosphonate (**2a**)*

It was obtained as a light yellow amorphous solid in 65 % yield (purified by silica gel column chromatography, using hexane/acetone 4:1 v/v as the eluting solvent): TLC $R_f = 0.45$ (hexane/acetone 4:1 v/v); mp: 73.1–74.6 °C. IR (ATR, cm^{-1}) $\bar{\nu}_{max}$ 2965, 2857, 2363, 1588, 1484, 1259, 1193, 1089, 911, 830, 771, 683, 538, 482. ^{1}H NMR (300 MHz, $CDCl_3$) δ 3.23–3.31 (4H, m, H-7, H-10), 3.55–3.62 (4H, m, H-8, H-9), 7.13–7.21 (4H, m, H-1, H-5), 7.25–7.34 (4H, m, H-2, H-4). ^{13}C NMR (75 MHz, $CDCl_3$) δ 44.93 (CH_2, C-7, C-10), 66.71 (CH_2, d, $J = 5.3$ Hz, C-8, C-9), 121.63 (CH, d, $J = 4.9$ Hz, C-1, C-5), 130.07 (CH, C-2, C-4), 130.80 (C, C-3), 149.29 (C, d, $J = 6.8$ Hz, C-6). GC–MS *m/z*: 387 $[M]^{+\cdot}$. HREIMS *m/z* ($M+H^+$): calcd for $C_{16}H_{16}Cl_2NO_4P$, 388.0267; found, 388.0158.

*Bis(4-nitrophenyl) morpholinophosphonate (**2b**)*

It was obtained as a white crystal in 11 % yield (purified by silica gel column chromatography, using hexane/ethyl acetate 1:1 v/v as the eluting solvent): TLC $R_f = 0.32$ (hexane/ethyl acetate 1:1 v/v); mp: 161.5–162.9 °C. IR (ATR, cm^{-1}) $\bar{\nu}_{max}$ 2858, 1588, 1513, 1342, 1199, 908, 846, 745, 471; ^{1}H NMR (300 MHz, $CDCl_3$) δ 3.30–3.38 (4H, m, H-7, H-10), 3.60–3.67 (4H, m, H-8, H-9), 7.38–7.45 (4H, m, H-1, H-5), 8.24–8.31 (4H, m, H-2, H-4). ^{13}C NMR

(75 MHz, $CDCl_3$) δ 44.67 (CH_2, C-7, C-10), 66.59 (CH_2, d, $J = 5.7$ Hz, C-8, C-9), 120.55 (CH, d, $J = 5.4$ Hz, C-1, C-5), 125.87 (CH, C-2, C-4), 144.95 (C, C-3), 155.04 (C, d, $J = 6.5$ Hz, C-6). GC–MS *m/z*: 409 $[M]^{+\cdot}$. HREIMS *m/z* ($M+H^+$): calcd for $C_{16}H_{16}N_3O_8P$, 410.0748; found, 410.0759.

*4-Chlorophenyl N,N′-diphenyl phosphate (**3a**)*

It was obtained as a colorless crystal in 38 % yield (purified by silica gel column chromatography, using hexane/ethyl acetate 1:1 v/v as the eluting solvent): TLC $R_f = 0.63$ (hexane/ethyl acetate 1:1 v/v); mp: 169.4–170.0 °C. IR (ATR, cm^{-1}) $\bar{\nu}_{max}$ 3374, 3142, 2980, 2906, 2367, 1600, 1476, 1394, 1298, 1204, 911, 845, 746, 686, 508. ^1H NMR (300 MHz, DMSO) δ 6.85 (2H, t, $J = 6.9$ Hz, –NH), 7.08–7.28 (10H, m, H-7, H-8, H-9, H-10, H-11), 7.42–7.46 (2H, m, H-1, H-5), 8.50 (2H, m, H-2, H-4). ^{13}C NMR (75 MHz, DMSO) δ 118.08 (CH, d, $J = 7.8$ Hz, C-7, C-11), 121.57 (CH, C-9), 122.97 (CH, d, $J = 4.7$ Hz, C-1, C-5), 129.44 (C, C-3), 129.65 (CH, C-8, C-10), 130.31 (CH, C-2, C-4), 141.32 (C, d, $J = 1.7$ Hz, C-12), 149.85 (C, d, $J = 6.3$ Hz, C-6). GC–MS *m/z*: 358 $[M]^{+\cdot}$. HREIMS *m/z* ($M+H^+$): calcd for $C_{18}H_{16}ClN_2O_2P$, 359.0711; found, 359.0607.

*4-Bromophenyl N,N′-diphenyl phosphate (**3b**)*

It was obtained as a colorless crystal in 16 % yield (purified by silica gel column chromatography, using hexane/ethyl acetate 2:1 v/v as the eluting solvent): TLC $R_f = 0.26$ (hexane/ethyl acetate 2:1 v/v); mp: 189.8–191.4 °C; IR (ATR, cm^{-1}) $\bar{\nu}_{max}$ 3362, 3139, 2906, 1476, 1203, 912, 745, 506. ^1H NMR (300 MHz, $CDCl_3$) δ 5.93 (2H, d, $J = 8.9$ Hz, –NH), 6.96–7.11 (8H, m, H-1, H-5, H-7, H-9, H-11), 7.18–7.38 (6H, m, H-2, H-4, H-8, H-10). ^{13}C NMR (75 MHz, $CDCl_3$) δ 118.59 (C, C-3), 118.69 (CH, C-7, C-11), 122.61 (CH, C-9), 122.69 (CH, C-1, C-5), 122.90 (CH, C-8, C-10), 129.67 (CH, C-2, C-4), 132.95 (C, C-12), 138.85 (C, C-6). GC–MS *m/z*: 402 $[M]^{+\cdot}$. HREIMS *m/z* ($M+H^+$): calcd for $C_{18}H_{16}BrN_2O_2P$, 403.0206; found, 403.0071.

*4-Chlorophenyl N,N′-dicyclohexylamidophosphinate (**4a**)*

It was obtained as an amorphous solid in 66 % yield (purified by silica gel column chromatography, using hexane/ethyl acetate 3:1 v/v as the eluting solvent): TLC $R_f = 0.12$ (hexane/ethyl acetate 3:1 v/v); mp: 106.6–107.6 °C; IR (ATR, cm^{-1}) $\bar{\nu}_{max}$ 3230, 2925, 2851, 1488, 1434, 1310, 1204, 1087, 1002, 888, 834, 754, 648, 648, 529, 486. ^1H NMR (300 MHz, $CDCl_3$) δ 0.97–2.00 (20H, m, –CH_2), 2.46 (2H, broad s, –NH), 3.0–3.15 (2H, m, H-12), 7.07–7.19 (2H, m, H-1, H-5), 7.20–7.35 (2H, m, H-2, H-4). ^{13}C NMR (75 MHz, $CDCl_3$) δ 25.31 (CH_2, C-8, C-10), 25.59 (CH_2, C-9), 36.18 (CH_2, t, $J = 5.0$ Hz, C-7, C-11), 50.86 (CH, C-12), 121.79 (CH, d, $J = 5.1$ Hz, C-1, C-5), 129.40 (C, C-3), 129.67 (CH, C-2, C-4), 150.28 (C, d, $J = 6.5$ Hz, C-6). GC–MS *m/z*: 370 $[M]^{+\cdot}$. HREIMS *m/z* ($M+H^+$): calcd for $C_{18}H_{28}ClN_2O_2P$, 371.1650; found, 371.1571.

*3-Chlorophenyl N,N′-dicyclohexylamidophosphinate (**4b**)*

It was obtained as a white amorphous solid in 6 % yield (purified by silica gel column chromatography, using hexane/ethyl acetate 1:1 v/v as the eluting solvent): TLC $R_f = 0.43$ (hexane/ethyl acetate 1:1 v/v); mp: 92.0–93.0 °C. IR (ATR, cm^{-1}) $\bar{\nu}_{max}$ 3377, 3176, 2927, 2851, 1589, 1424, 1207, 1092, 1017, 930, 774, 666, 526. ^1H NMR (300 MHz, $CDCl_3$) δ 1.02–1.99 (20H, m, –CH_2), 2.50 (2H, broad s, –NH), 3.0–3.17 (2H, m, H-12), 7.04–7.31 (4H, m, H-1, H-2, H-3, H-5). ^{13}C NMR (75 MHz, $CDCl_3$) δ 25.31 (CH_2, C-8, C-10), 25.59 (CH_2, C-9), 36.15 (CH_2, t, $J = 4.5$ Hz, C-7, C-11), 50.90 (CH, C-12), 118.80 (CH, d, $J = 4.9$ Hz, C-5), 121.02 (CH, d, $J = 5.4$ Hz, C-1), 124.51 (CH, C-3), 130.43 (CH, C-2), 134.85 (C, C-4), 152.28 (C, d, $J = 6.3$ Hz, C-6). GC–MS *m/z*: 370 $[M]^{+\cdot}$. HREIMS *m/z* ($M+H^+$): calcd for $C_{18}H_{28}ClN_2O_2P$, 371.1650; found, 371.1574.

*2-Bromophenyl N,N′-dicyclohexylamidophosphinate (**4c**)*

It was obtained as a white solid in 36 % yield (purified by silica gel column chromatography, using hexane/ethyl acetate 2:1 v/v as the eluting solvent): TLC $R_f = 0.22$ (hexane/ethyl acetate 2:1 v/v); mp: 111.6–113.2 °C; IR (ATR, cm^{-1}) $\bar{\nu}_{max}$ 3208, 2928, 2850, 1474, 1219, 1087, 908, 756, 506. ^1H NMR (300 MHz, $CDCl_3$) δ 1.20–2.03 (20H, m, –CH_2), 2.69 (2H, t, $J = 9.9$ Hz, –NH), 3.05–3.25 (2H, m, H-12), 6.94–7.00 (1H, m, H-3), 7.21–7.27 (1H, m, H-2), 7.50–7.58 (2H, m, H-1, H-4). ^{13}C NMR (75 MHz, $CDCl_3$) δ 25.04 (CH_2, C-8, C-10), 25.34 (CH_2, C-9), 35.88 (CH_2, d, $J = 4.8$ Hz, C-7, C-11), 50.55 (CH, C-12), 114.47 (C, C-5), 121.86 (CH, d, $J = 2.9$ Hz, C-1), 125.18 (CH, C-3), 128.59 (CH, C-2), 133.11 (CH, C-4), 148.61 (C, d, $J = 6.0$ Hz, C-6). GC–MS *m/z*: 416 $[M]^{+\cdot}$. HREIMS *m/z* ($M+H^+$): calcd for $C_{18}H_{28}BrN_2O_2P$, 415.1145; found, 415.0993.

*4-Fluorophenyl N,N′-dicyclohexylamidophosphinate (**4d**)*

It was obtained as a white amorphous solid in 28 % yield (purified by silica gel column chromatography, using hexane/ethyl acetate 2:1 v/v as the eluting solvent): TLC $R_f = 0.39$ (hexane/ethyl acetate 2:1 v/v); mp 117.9–119.3 °C; IR (ATR, cm^{-1}) $\bar{\nu}_{max}$ 3232, 2926, 2853, 1503, 1435, 1198, 1087, 892,

812, 484. ^{1}H NMR (300 MHz, $CDCl_3$) δ 1.03–1.97 (20H, m, –C<u>H</u>$_2$), 2.53 (2H, t, J = 2.4 Hz, –N<u>H</u>), 2.99–3.16 (2H, m, H-12), 6.92–7.02 (2H, m, H-2, H-4), 7.13–7.21 (2H, m, H-1, H-5). ^{13}C NMR (75 MHz, $CDCl_3$) δ 25.05 (CH_2, C-8, C-10), 25.34 (CH_2, C-9), 35.94 (CH_2, C-7, C-11), 50.58 (CH, C-12), 115.93 (CH, d, J = 23.2 Hz, C-2, C-4), 121.48 (CH, q, J = 4.8 Hz and J = 8.2 Hz, C-1, C-5), 147.31 (C, q, J = 2.1 Hz and J = 6.2 Hz, C-6), 159.11 (C, d, J = 240.8 Hz, C-3). GC–MS m/z: 354 $[M]^{+\cdot}$. HREIMS m/z ($M+H^+$): calcd for $C_{18}H_{28}FN_2O_2P$, 355.1945; found, 355.1963.

*Bis(4-chlorophenyl) cyclohexylphosphoramidate (**5a**)*

It was obtained as a colorless solid in 40 % yield (purified by silica gel column chromatography, using hexane/ethyl acetate 3:1 v/v as the eluting solvent): TLC R_f = 0.60 (hexane/ethyl acetate 3:1 v/v); mp: 123.7–124.2 °C. IR (ATR, cm^{-1}) $\bar{\nu}_{max}$ 3192, 2933, 2854, 1589, 1483, 1201, 1092, 1014, 918, 834, 770, 661, 519. ^{1}H NMR (300 MHz, $CDCl_3$) δ 1.06–1.93 (11H, m, –C<u>H</u>$_2$, H-12), 3.17–3.22 (1H, m, –N<u>H</u>), 7.15–7.22 (4H, m, H-1, H-5), 7.28–7.32 (4H, m, H-2, H-4). ^{13}C NMR (75 MHz, $CDCl_3$) δ 25.14 (CH_2, C-8, C-10), 25.43 (CH_2, C-9), 35.67 (CH_2, d, J = 5.0 Hz, C-7, C-11), 51.56 (CH, C-12), 121.73 (CH, d, J = 5.1 Hz, C-1, C-5), 129.91 (CH, C-2, C-4), 130.48 (C, C-3), 149.56 (C, d, J = 6.9 Hz, C-6). GC–MS m/z: 399 $[M]^{+\cdot}$. HREIMS m/z ($M+H^+$): calcd for $C_{18}H_{20}Cl_2NO_3P$, 400.0631; found, 400.0520.

*Bis(3-chlorophenyl) cyclohexylphosphoramidate (**5b**)*

It was obtained as a white amorphous solid in 22 % yield (purified by silica gel column chromatography, using hexane/ethyl acetate 4:1 v/v as the eluting solvent): TLC R_f = 0.28 (hexane/ethyl acetate 4:1 v/v); mp: 89.3–89.7 °C. IR (ATR, cm^{-1}) $\bar{\nu}_{max}$ 3184, 2933, 2850, 1584, 1468, 1249, 1199, 1112, 940, 776, 674, 613. ^{1}H NMR (300 MHz, $CDCl_3$) δ 1.09–1.93 (11H, m, –C<u>H</u>$_2$, H-12), 3.07–3.29 (1H, m, –N<u>H</u>), 7.10–7.34 (8H, m, H-1, H-2, H-3, H-5). ^{13}C NMR (75 MHz, $CDCl_3$) δ 25.13 (CH_2, C-8, C-10), 25.43 (CH_2, C-9), 35.65 (CH_2, d, J = 5.0 Hz, C-7, C-11), 51.62 (CH, C-12), 118.7 (CH, d, J = 4.9 Hz, C-5), 121.02 (CH, d, J = 5.5 Hz, C-1), 125.53 (CH, C-3), 130.65 (CH, C-2), 135.13 (C, C-4), 151.45 (C, d, J = 7.0 Hz, C-6). GC–MS m/z: 399 $[M]^{+\cdot}$. HREIMS m/z ($M+H^+$): calcd for $C_{18}H_{20}Cl_2NO_3P$, 400.0631; found, 400.0530.

*Bis(4-bromophenyl) cyclohexylphosphoramidate (**5c**)*

It was obtained as a light yellow amorphous solid in 8 % yield (purified by silica gel column chromatography, using hexane/ethyl acetate 2:1 v/v as the eluting solvent): TLC R_f = 0.46 (hexane/ethyl acetate 2:1 v/v); mp: 143.5–144.9 °C; IR (ATR, cm^{-1}) $\bar{\nu}_{max}$ 3177, 2929, 2855, 1583, 1481, 1197, 915, 830, 737, 521. ^{1}H NMR (300 MHz, $CDCl_3$) δ 1.04–1.94 (10H, m, –C<u>H</u>$_2$), 2.99 (1H, t, J = 12.3 Hz, –N<u>H</u>), 3.06–3.27 (1H, m, H-12), 7.09–7.16 (4H, m, H-1, H-5), 7.40–7.47 (4H, m, H-2, H-4). ^{13}C NMR (75 MHz, $CDCl_3$) δ 24.87 (CH_2, C-8, C-10), 25.17 (CH_2, C-9), 35.44 (CH_2, d, J = 5.1 Hz, C-7, C-11), 51.31 (CH, C-12), 117.85 (C, C-3), 121.89 (CH, d, J = 5.1 Hz, C-1, C-5), 132.65 (CH, C-2, C-4), 149.83 (C, d, J = 6.9 Hz, C-6). GC–MS m/z: 487 $[M]^{+\cdot}$. HREIMS m/z ($M+H^+$): calcd for $C_{18}H_{20}Br_2NO_3P$, 487.9620; found, 487.9512.

*Bis(4-nitrophenyl) cyclohexylphosphoramidate (**5d**)*

It was obtained as a white solid in 12 % yield (purified by silica gel column chromatography, using hexane/ethyl acetate 3:1 v/v as the eluting solvent): TLC R_f = 0.31 (hexane/ethyl acetate 3:1 v/v); mp: 175.4–176.7 °C. IR (ATR, cm^{-1}) $\bar{\nu}_{max}$ 3157, 2926, 2851, 1589, 1512, 1341, 1207, 1105, 920, 854, 748, 618, 532. ^{1}H NMR (300 MHz, $CDCl_3$) δ 1.16–1.90 (10H, m, –C<u>H</u>$_2$), 3.15–3.37 (2H, m, –N<u>H</u>, H-12), 7.39–7.44 (4H, m, H-1, H-5), 8.22–8.28 (4H, m, H-2, H-4). ^{13}C NMR (75 MHz, $CDCl_3$) δ 24.79 (CH_2, C-8, C-10), 25.02 (CH_2, C-9), 35.37 (CH_2, d, J = 5.1 Hz, C-7, C-11), 51.64 (CH, C-12), 120.58 (CH, d, J = 5.6 Hz, C-1, C-5), 125.74 (CH, C-2, C-4), 144.73 (C, C-3), 155.55 (C, d, J = 6.4 Hz, C-6). GC–MS m/z: 421 $[M]^{+\cdot}$. HREIMS m/z ($M+H^+$): calcd for $C_{18}H_{20}N_3O_7P$, 422.1112; found, 422.1027.

*4-Bromophenyl 4,4′-dimethyl-(N,N′-diphenyl) phosphate (**6a**)*

It was obtained as a white amorphous solid in 13 % yield (purified by silica gel column chromatography, using hexane/ethyl acetate 2:1 v/v as the eluting solvent): TLC R_f = 0.51 (hexane/ethyl acetate 2:1 v/v); mp: 104.7–106.1 °C; IR (ATR, cm^{-1}) $\bar{\nu}_{max}$ 3377, 3139, 1616, 1482, 1202, 991, 817, 493. ^{1}H NMR (300 MHz, $CDCl_3$) δ 1.67 (6H, s, –C<u>H</u>$_3$), 6.48–6.65 (10H, m, H-1, H-5, H-7, H-8, H-10, H-11), 6.88–6.92 (2H, m, H-2, H-4), 7.32 (2H, d, J = 9.9 Hz, –N<u>H</u>). ^{13}C NMR (75 MHz, $CDCl_3$) δ 19.44 (CH_3, C-13), 116.18 (C, C-3), 116.88 (CH, d, J = 7.4 Hz, C-7, C-11), 121.71 (CH, d, J = 4.6 Hz, C-1, C-5), 128.35 (C, C-9), 129.19 (CH, C-8, C-10), 131.20 (CH, C-2, C-4), 136.68 (C, C-12), 148.75 (C, d, J = 6.4 Hz, C-6). GC–MS m/z: 430 $[M]^{+\cdot}$. HREIMS m/z ($M+H^+$): calcd for $C_{20}H_{20}BrN_2O_2P$, 431.0519; found, 431.0532.

*4-Chlorophenyl N,N,N′,N′-tetraethyldiamidophosphinate (**7a**)*

It was obtained as a light yellow oil in 38 % yield (purified by silica gel column chromatography, using hexane/ethyl

acetate 3:1 v/v as the eluting solvent): TLC $R_f = 0.33$ (hexane/ethyl acetate 3:1 v/v); IR (ATR, cm^{-1}) $\bar{\nu}_{max}$ 2972, 2933, 2874, 1592, 1486, 1380, 1163, 1091, 1025, 897, 763, 541. ^1H NMR (300 MHz, $CDCl_3$) δ 1.07 (12H, t, $J = 7.2$ Hz, –C<u>H</u>$_3$), 3.10 (8H, dq, $J = 7.2$ Hz and $J = 3.0$ Hz, –C<u>H</u>$_2$), 7.12–7.19 (2H, m, H-1, H-5), 7.21–7.28 (2H, m, H-2, H-4). ^{13}C NMR (75 MHz, $CDCl_3$) δ 14.32 (CH_3, d, $J = 2.2$ Hz, C-8), 39.95 (CH_2, d, $J = 11.4$ Hz, C-7), 121.76 (CH, d, $J = 5.3$ Hz, C-1, C-5); 129.14 (C, C-3), 129.70 (CH, C-2, C-4), 150.40 (C, d, $J = 6.0$ Hz, C-6). GC–MS *m/z*: 318 $[M]^{+\cdot}$. HREIMS *m/z* ($M+H^+$): calcd for $C_{14}H_{24}ClN_2O_2P$, 319.1337; found, 319.1235.

*4-Bromophenyl N,N,N′,N′-tetraethyldiamidophosphinate (**7b**)*

It was obtained as a light yellow oil in 13 % yield (purified by silica gel column chromatography, using hexane/ethyl acetate 2:1 v/v as the eluting solvent): TLC $R_f = 0.33$ (hexane/ethyl acetate 2:1 v/v); IR (ATR, cm^{-1}) $\bar{\nu}_{max}$ 2971, 2922, 2877, 1482, 1206, 1163, 893, 830, 718. ^1H NMR (300 MHz, $CDCl_3$) δ 0.99–1.13 (12H, m, –C<u>H</u>$_3$), 3.04–3.20 (8H, m, –C<u>H</u>$_2$), 7.06–7.15 (2H, m, H-1, H-5), 7.36–7.46 (2H, m, H-2, H-4). ^{13}C NMR (75 MHz, $CDCl_3$) δ 14.33 and 13.90 (CH_3, d, $J = 2.2$ Hz, C-8), 40.08 and 39.86 (CH_2, d, $J = 4.7$ Hz, C-7), 118.16 and 116.73 (C, C-3), 122.28 and 122.20 (CH, d, $J = 2.4$ Hz, C-1, C-5), 132.81 and 132.56 (CH, C-2, C-4), 149.76 and 150.96 (C, d, $J = 5.8$ Hz, C-6). GC–MS *m/z*: 362 $[M]^{+\cdot}$. HREIMS *m/z* ($M+H^+$): calcd for $C_{14}H_{24}BrN_2O_2P$, 363.0832; found, 363.0743.

*4-Fluorophenyl N,N,N′,N′-tetraethyldiamidophosphinate (**7c**)*

It was obtained as a white crystal in 25 % yield (purified by silica gel column chromatography, using hexane/ethyl acetate 3:1 v/v as the eluting solvent): TLC $R_f = 0.53$ (hexane/ethyl acetate 3:1 v/v); IR (ATR, cm^{-1}) $\bar{\nu}_{max}$ 2973, 1501, 1380, 1168, 1025, 900, 817, 500. ^1H NMR (300 MHz, $CDCl_3$) δ 1.07 (12H, t, $J = 7.2$ Hz, –C<u>H</u>$_3$), 3.11 (8H, dq, $J = 7.2$ Hz and $J = 18.3$ Hz, –C<u>H</u>$_2$), 6.91–7.03 (2H, m, H-2, H-4), 7.13–7.20 (2H, m, H-1, H-5). ^{13}C NMR (75 MHz, $CDCl_3$) δ 14.05 (CH_3, d, $J = 2.1$ Hz, C-8), 39.63 (CH_2, d, $J = 4.7$ Hz, C-7), 115.97 (CH, d, $J = 23.0$ Hz, C-2, C-4), 121.43 (CH, q, $J = 4.8$ Hz and $J = 8.1$ Hz, C-1, C-5), 147.43 (C, C-6), 158.96 (C, d, $J = 239.9$ Hz, C-3). GC–MS *m/z*: 302 $[M]^{+\cdot}$. HREIMS *m/z* ($M+H^+$): calcd for $C_{14}H_{24}FN_2O_2P$, 303.1632; found, 303.1653.

*Bis(3-chlorophenyl) N,N-diethyldiamidophosphinate (**8a**)*

It was obtained as a light yellow oil in 13 % yield (purified by silica gel column chromatography, using hexane/ethyl acetate 3:1 v/v as the eluting solvent): TLC $R_f = 0.36$ (hexane/ethyl acetate 3:1 v/v); IR (ATR, cm^{-1}) $\bar{\nu}_{max}$ 2975, 1584, 1469, 1262, 1198, 1037, 925, 775, 676, 602, 541. ^1H NMR (300 MHz, $CDCl_3$): δ 1.07 (6H, t, $J = 7.1$ Hz, –C<u>H</u>$_3$), 3.23 (4H, dq, $J = 12.4$ Hz and $J = 7.1$ Hz, –C<u>H</u>$_2$), 7.31–7.64 (8H, m, H-1, H-2, H-3, H-5). ^{13}C NMR (75 MHz, $CDCl_3$): δ 8.68 (CH_3, C-8), 46.78 (CH_2, C-7), 121.39–121.97 (CH, m, C-5), 129.71–129.84 (CH, m, C-1), 130.19–130.36 (CH, m, C-3), 132.52–133.10 (CH, m, C-2), 147.85–148.04 (C, m, C-4), 148.38–148.66 (C, m, C-6). GC–MS *m/z*: 373 $[M]^{+\cdot}$. HREIMS *m/z* ($M+H^+$): calcd for $C_{16}H_{18}Cl_2NO_3P$, 374.0474; found, 374.0383.

*4-Chlorophenyl N,N′-dipiperidin-1-ilphosphinate (**9a**)*

It was obtained as a light yellow oil in 85 % yield (purified by silica gel column chromatography, using hexane/ethyl acetate 3:1 v/v as the eluting solvent): TLC $R_f = 0.23$ (hexane/ethyl acetate 3:1 v/v); IR (ATR, cm^{-1}) $\bar{\nu}_{max}$ 2932, 2849, 1720, 1592, 1486, 1339, 1204, 1160, 1071, 956, 898, 832, 729, 565, 479. ^1H NMR (300 MHz, $CDCl_3$): δ 1.39–1.65 (12H, m, H-8, H-9, H-10), 3.05–3.15 (8H, m, H-7, H-11), 7.11–7.19 (2H, m, H-1, H-5), 7.22–7.34 (2H, m, H-2, H-4). ^{13}C NMR (75 MHz, $CDCl_3$): δ 24.71 (CH_2, C-9), 26.30 (CH_2, d, $J = 5.6$ Hz, C-8, C-10), 45.77 (CH_2, d, $J = 2.7$ Hz, C-7, C-11), 121.78 (CH, d, $J = 5.3$ Hz, C-1, C-5), 129.27 (C, C-3), 129.65 (CH, C-2, C-4), 150.46 (C, C-6). GC–MS *m/z*: 342 $[M]^{+\cdot}$. HREIMS *m/z* ($M+H^+$): calcd for $C_{16}H_{22}ClN_2O_2P$, 343.1337; found, 343.1211.

*3-Chlorophenyl N,N′-dipiperidin-1-ilphosphinate (**9b**)*

It was obtained as a light yellow oil in 91 % yield (purified by silica gel column chromatography, using hexane/ethyl acetate 1:1 v/v as the eluting solvent): TLC $R_f = 0.35$ (hexane/ethyl acetate 1:1 v/v); IR (ATR, cm^{-1}) $\bar{\nu}_{max}$ 2934, 2849, 1588, 1472, 1339, 1070, 923, 730, 680, 475. ^1H NMR (300 MHz, $CDCl_3$): δ 1.39–1.61 (12H, m, H-8, H-9, H-10), 3.04–3.21 (8H, m, H-7, H-11), 7.05–7.32 (4H, m, H-1, H-2, H-3, H-5). ^{13}C NMR (75 MHz, $CDCl_3$): δ 24.71 (CH_2, C-9), 26.29 (CH_2, d, $J = 5.3$ Hz, C-8, C-10), 45.78 (CH_2, d, $J = 2.3$ Hz, C-7, C-11), 118.73 (CH, d, $J = 5.0$ Hz, C-5), 120.97 (CH, d, $J = 5.5$ Hz, C-1), 124.38 (CH, C-3), 130.41 (CH, C-2), 134.82 (C, C-4), 152.45 (C, d, $J = 6.1$ Hz, C-6). GC–MS *m/z*: 342 $[M]^{+\cdot}$. HREIMS *m/z* ($M+H^+$): calcd for $C_{16}H_{24}ClN_2O_2P$, 343.1337; found, 343.1226.

*4-Bromophenyl N,N′-dipiperidin-1-ilphosphinate (**9c**)*

It was obtained as a light yellow oil in 32 % yield (purified by silica gel column chromatography, using hexane/ethyl acetate 2:1 v/v as the eluting solvent): TLC $R_f = 0.30$ (hexane/ethyl acetate 2:1 v/v); IR (ATR, cm^{-1}) $\bar{\nu}_{max}$ 2932, 2849, 1719, 1528, 1482, 1339, 1219, 1199, 1157, 1113, 1065, 1027, 1009, 956, 904, 830, 758, 729, 631, 608, 560, 473. ^{1}H NMR (300 MHz, $CDCl_3$): δ 1.39–1.61 (12H, m, H-8, H-9, H-10), 3.03–3.15 (8H, m, H-7, H-11), 7.06–7.15 (2H, m, H-1, H-5), 7.35–7.45 (2H, m, H-2, H-4). ^{13}C NMR (75 MHz, $CDCl_3$): δ 24.69 (CH_2, C-9), 26.29 (CH_2, d, $J = 2.4$ Hz, C-8, C-10), 45.77 (CH_2, d, $J = 2.4$ Hz, C-7, C-11), 116.93 (C, C-3), 122.26 (CH, d, $J = 2.4$ Hz, C-1, C-5), 132.64 (CH, C-2, C-4), 150.92 (C, d, $J = 6.2$ Hz, C-6). GC–MS *m/z*: 386 $[M]^{+\cdot}$. HREIMS *m/z* ($M+H^+$): calcd for $C_{16}H_{24}BrN_2O_2P$, 387.0832; found, 387.0777.

*4-Fluorophenyl N,N′-dipiperidin-1-ilphosphinate (**9d**)*

It was obtained as a light yellow oil in 30 % yield (purified by silica gel column chromatography, using hexane/ethyl acetate 3:1 v/v as the eluting solvent): TLC $R_f = 0.51$ (hexane/ethyl acetate 3:1 v/v); IR (ATR, cm^{-1}) $\bar{\nu}_{max}$ 2933, 2849, 1501, 1339, 1193, 1071, 903, 817, 733, 477. ^{1}H NMR (300 MHz, $CDCl_3$): δ 1.42–1.59 (12H, m, H-8, H-9, H-10), 3.06–3.13 (8H, m, H-7, H-11), 6.93–7.01 (2H, m, H-2, H-4), 7.13–7.19 (2H, m, H-1, H-5). ^{13}C NMR (75 MHz, $CDCl_3$): δ 24.44 (CH_2, C-9), 26.04 (CH_2, d, $J = 5.3$ Hz, C-7, C-11), 45.49 (CH_2, d, $J = 2.3$ Hz, C-8, C-10); 115.87 (CH, d, $J = 23.1$ Hz, C-2, C-4), 121.41 (CH, q, $J = 4.8$ Hz and $J = 8.3$ Hz, C-1, C-5), 147.40 (C, C-6), 158.99 (C, d, $J = 240.8$ Hz, C-3). GC–MS *m/z*: 326 $[M]^{+\cdot}$. HREIMS *m/z* ($M+H^+$): calcd for $C_{16}H_{24}FN_2O_2P$, 327.1632; found, 327.1663.

*Bis(4-chlorophenyl)piperidin-1-ilphosphonate (**10a**)*

It was obtained as a light yellow oil in 64 % yield (purified by silica gel column chromatography, using hexane/ethyl acetate 3:1 v/v as the eluting solvent): TLC $R_f = 0.74$ (hexane/ethyl acetate 3:1 v/v); IR (ATR, cm^{-1}) $\bar{\nu}_{max}$ 3096, 2937, 2854, 1589, 1484, 1269, 1194, 1089, 908, 829, 769, 638, 479. ^{1}H NMR (300 MHz, $CDCl_3$): δ 1.39–1.60 (6H, m, H-8, H-9, H-10), 3.15–3.29 (4H, m, H-7, H-11), 7.13–7.25 (4H, m, H-1, H-5), 7.26–7.35 (4H, m, H-2, H-4). ^{13}C NMR (75 MHz, $CDCl_3$): δ 24.33 (CH_2, C-9), 25.93 (CH_2, d, $J = 4.5$ Hz, C-8, C-10), 45.84 (CH_2, d, $J = 2.2$ Hz, C-7, C-11), 121.69 (CH, d, $J = 5.4$ Hz, C-1, C-5), 129.92 (C, C-3), 130.41 (CH, C-2, C-4), 149.59 (C, d, $J = 6.4$ Hz, C-6). GC–MS *m/z*: 385 $[M]^{+\cdot}$. HREIMS *m/z* ($M+H^+$): calcd for $C_{17}H_{18}Cl_2NO_3P$, 386.0474; found, 386.0368.

*3-Chlorophenyl N,N′-dimorfolin-1-ilphosphinate (**11a**)*

It was obtained as a colorless oil in 52 % yield (purified by silica gel column chromatography, using hexane/acetone 1:1 v/v as the eluting solvent): TLC $R_f = 0.40$ (hexane/acetone 1:1 v/v); mp: IR (ATR, cm^{-1}) $\bar{\nu}_{max}$ 2967, 2916, 2854, 1700, 1589, 1212, 1112, 930, 735, 503. ^{1}H NMR (300 MHz, $CDCl_3$): δ 3.12–3.29 (8H, m, H-7, H-10), 3.54–3.73 (8H, m, H-8, H-9), 7.09–7.33 (4H, m, H-1, H-2, H-3, H-5). ^{13}C NMR (75 MHz, $CDCl_3$): δ 44.99 (CH_2, C7, C-10), 67.20 (CH_2, d, $J = 5.8$ Hz, C-8, C-9), 118.57 (CH, d, $J = 4.8$ Hz, C-5), 120.87 (CH, d, $J = 5.5$ Hz, C-1), 125.10 (CH, C-3), 130.71 (CH, C-2), 135.18 (C, C-4), 151.80 (C, d, $J = 6.0$ Hz, C-6). GC–MS *m/z*: 346 $[M]^{+\cdot}$. HREIMS *m/z* ($M+H^+$): calcd for $C_{14}H_{20}ClN_2O_4P$, 347.0922; found, 347.0841.

*4-Bromophenyl N,N′-dimorfolin-1-ilphosphinate (**11b**)*

It was obtained as a white crystal in 46 % yield (purified by silica gel column chromatography, using hexane/ethyl acetate 3:1 v/v as the eluting solvent): TLC $R_f = 0.60$ (hexane/ethyl acetate 3:1 v/v); mp. 112.7–113.9 °C. IR (ATR, cm^{-1}) $\bar{\nu}_{max}$ 2956, 2846, 1482, 1232, 1111, 967, 904, 840, 734, 473. ^{1}H NMR (300 MHz, $CDCl_3$): δ 3.15–3.22 (8H, m, H-7, H-10), 3.59–3.61 (8H, m, H-8, H-9), 7.09–7.15 (2H, m, H-1, H-5), 7.41–7.47 (2H, m, H-2, H-4). ^{13}C NMR (75 MHz, $CDCl_3$): δ 44.74 (CH_2, C-7, C-10), 66.96 (CH_2, d, $J = 5.8$ Hz, C-8, C-9) 117.37 (C, C-3), 121.83 (CH, d, $J = 5.0$ Hz, C-1, C-5), 132.68 (CH, C-2, C-4), 150.09 (C, d, $J = 5.9$ Hz, C-6). GC–MS *m/z*: 390 $[M]^{+\cdot}$. HREIMS *m/z* ($M+H^+$): calcd for $C_{14}H_{20}BrN_2O_4P$, 391.0417; found, 391.0281.

*4-Fluorophenyl N,N′-dimorfolin-1-ilphosphinate (**11c**)*

It was obtained as a white crystal in 55 % yield (purified by silica gel column chromatography, using hexane/ethyl acetate 3:1 v/v as the eluting solvent): TLC $R_f = 0.57$ (hexane/ethyl acetate 3:1 v/v); mp. 128.7–130.1 °C. IR (ATR, cm^{-1}) $\bar{\nu}_{max}$ 2974, 2851, 1502, 1230, 1109, 965, 907, 843, 741, 489. ^{1}H NMR (300 MHz, $CDCl_3$): δ 3.14–3.23 (8H, m, H-7, H-10), 3.58–3.65 (8H, m, H-8, H-9), 6.97–7.05 (2H, m, H-2, H-4), 7.13–7.21 (2H, m, H-1, H-5). ^{13}C NMR (75 MHz, $CDCl_3$): δ 44.72 (CH_2, C-7, C-10), 66.94 (CH_2, d, $J = 5.8$ Hz, C-8, C-9), 116.22 (CH, d, $J = 23.3$ Hz, C-2, C-4), 121.35 (CH, q, $J = 4.9$ Hz and $J = 8.4$ Hz, C-1, C-5), 146.82 (C, q, $J = 2.8$ Hz and $J = 5.8$ Hz, C-6), 159.31 (C, d, $J = 241.8$, C-3). GC–MS *m/z*: 330 $[M]^{+\cdot}$. HREIMS *m/z* ($M+H^+$): calcd for $C_{14}H_{20}FN_2O_4P$, 331.1217; found, 331.1160.

Urease inhibition assay

The screening for identifying potential urease inhibitors was done by incubating each synthesized compound at final concentration of 1.6 mM in reactions containing buffer solution (Na_2HPO_4/NaH_2PO_4 50 mM, pH 7.4), urea (10 or 20 mM), and 1.25×10^{-2} U of urease (Sigma U-1500-100 kU). Each mixture was incubated for 15 min at 25 °C, and the reactions were interrupted following the methodology described by Weatherburn (1967). The ammonium concentration was determined by phenol hypochloride assay (636 nm), and the inhibition percentage [INH(%)] was calculated by the following equation: $INH(\%) = 100 - ((A_{INH}/A_B) \times 100)$. In this equation, A_{INH} and A_B are ammonium concentration in the tubes with and without inhibitor, respectively. The inhibitory potential of the phosphoramidates was compared to those of the standard inhibitors HU and TU. The phosphoramidates that were able to inhibit urease activity by over 40 % were further used from 50 to 3,200 μM to determine the concentration necessary to inhibit the enzyme by 50 % (IC_{50}). All experiments were performed in triplicate. The cluster analysis was performed by employing unweighted pair-group average as amalgamation (joining) rule and city-block (Manhattan) distances as distance metric.

Quantum chemical and physicochemical parameters

The physicochemical parameters were determined using the online software provided by Molinspiration Cheminformatics (Bratislava, Slovak Republic). Molecular attributes analyzed were *n*-octanol/water partition coefficient (*c*Log*P*), the amount of hydrogen bond donors (HBD), the amount of HBA, the molecular weight of the compounds (MW), nRotb, and total polar surface area (TPSA). The values of the TPSA were determined using the above software employing the method described by Ertl *et al*., (2000), and it was used to calculate the percentage of absorption (%ABS) according to the following equation: $\%ABS = 109 - 0.345 \times TPSA$, as reported (Ertl *et al.*, 2000).

Quantum mechanical calculations for compounds of the series **2**–**11** were performed using the Spartan 10 (Hehre and Ohlinger, 2010) and the Gaussian 09 (Frisch *et al*., 2009) programs. Computational geometry optimizations were carried out with the Spartan 10 software package employing semi-empirical PM6 method. The most stable conformers were fully optimized with at the B3LYP/6-31G(*d*,*p*) level of theory, where B3LYP is Becke three-parameter exchange functional, combined with the Lee–Yang–Parr correlation functional, at gas phase (Becke, 1993). The DFT/B3LYP method is recommended for the estimation of molecular properties related to reactivity of molecules, such as the energy of the highest occupied molecular orbital (E_{HOMO}) and the energy of the lowest unoccupied molecular orbital (E_{LUMO}) (Zhang and Musgrave, 2007). Predictions of the HOMO–LUMO energies and dipole moment were performed in DFT energy calculations (B3LYP/6-311++G(2*d*,*p*)) considering the SMD solvation model and water as solvent (Marenich *et al.*, 2009). Electrostatic potentials and HOMO/LUMO maps were calculated for the geometries fully optimized that resulted from DFT calculations using Gaussian 09 at the B3LYP/6-311++G(2*d*,*p*).

Conclusions

In summary, 25 new phosphoramidates were prepared and evaluated for their inhibitory activity against urease. Of these compounds, **5c** appeared the most promising, with good activity as urease inhibitors. The ADMET properties predicted for these phosphoramidates are in accordance with the general requirements for potential drugs, confirming that these compounds possess physicochemical properties that qualify them to have good pharmacokinetics and drug bioavailability. In addition, no violations of Lipinski's rule were observed for the majority of the phosphoramidates. The structure–activity relationships suggested that the presence of cyclohexylamine group seems to increase the biological activity of the compounds. The promising biological results obtained, along with the good drug-likeness predictors that were calculated, make these compounds valid leads for further studies in therapies that require compounds with inhibitory activity ureolitic and for synthesizing new phosphoramidates which might be serve as a valuable prototype with improved potency.

Acknowledgments We are grateful to the following Brazilian agencies: Conselho Nacional de Desenvolvimento Científico e Tecnológico (CNPq) for research fellowships (AJD, CRAM, LCAB), Fundação de Amparo à Pesquisa de Minas Gerais (FAPEMIG), Coordenação de Aperfeiçoamento de Pessoal de Nível Superior (CAPES) and FINEP for financial support. We also thanks to Dr. Adão Sabino and Mr. Augusto Carvalho for obtaining the high resolution mass spectra.

References

Alafeefy AM, Alqasoumi SI, Ashour AE, Masand V, Al-Jaber NA, Ben Hadda T, Mohamed MA (2012) Quinazoline-tyrphostin as a new class of antitumor agents, molecular properties prediction, synthesis and biological testing. Eur J Med Chem 53:133–140

Amtul Z, Rahman AU, Siddiqui RA, Choudhary MI (2002) Chemistry and mechanism of urease inhibition. Curr Med Chem 9:1323–1348

Arantes FFP, Barbosa LCA, Maltha CRA, Demuner AJ, Fidêncio PH, Carneiro JWM (2011) A quantum chemical and chemometric study of sesquiterpene lactones with cytotoxicity against tumor cells. J Chemom 25:401–407

Becke AD (1993) Density-functional thermochemistry. III. The role of exact exchange. J Chem Phys 98:5648–5652

Borrello L, Chiacchio U, Corsaro A, Pistarà V, Iannazzo D (2009) Phosphoroamidate derivatives of *N*, *O*-nucleosides as inhibitors of reverse transcriptase. Arkivoc 2009:112–124

Correa-Basurto J, Flores-Sandoval C, Marin-Cruz J, Rojo-Dominguez A, Espinoza-Fonseca LM, Trujillo-Ferrara JG (2007) Docking and quantum mechanic studies on cholinesterases and their inhibitors. Eur J Med Chem 42:10–19

Cramer F, Hennrich N, Imidoester V (1961) Die Umlagerung von Trichloracetimidaten zu N-substituierten Säureamiden. Chem Ber 94:976–989

de Oliveira DB, Gaudio AC (2001) BuildQSAR: a new computer program for QSAR analysis. Quant Struct Act Relat 19:599–601

Derudas M, Carta D, Brancale A, Vanpouille C, Lisco A, Margolis L, Balzarini J, McGuigan C (2009) The application of phosphoramidate protide technology to acyclovir confers anti-HIV inhibition. J Med Chem 52:5520–5530

Derudas M, Brancale A, Naesens L, Neyts J, Balzarini J, McGuigan C (2010) Application of the phosphoramidate ProTide approach to the antiviral drug ribavirin. Bioorg Med Chem 18:2748–2755

Donghi M, Attenni B, Gardelli C, Marco AD, Fiore F, Giuliano C, Laufer R, Leone JF, Pucci V, Rowley M, Narjes F (2009) Synthesis and evaluation of novel phosphoramidate prodrugs of 2′-methyl cytidine as inhibitors of hepatitis C virus NS5B polymerase. Bioorg Med Chem Lett 19:1392–1395

Duckworth MJ, Okoli AS, Mendz GL (2009) Novel *Helicobacter pylori* therapeutic targets: the unusual suspects. Expert Rev Anti Infect Ther 7:835–867

Ertl P, Rohde B, Selzer P (2000) Fast calculation of molecular polar surface area as a sum of fragment-based contributions and its application to the prediction of drug transport properties. J Med Chem 43:3714–3717

Follmer C (2010) Ureases as a target for the treatment of gastric and urinary infections. J Clin Pathol 63:424–430

Frisch MJ, Trucks GW, Schlegel HB, Scuseria GE, Robb MA, Cheeseman JR, Scalmani G, Barone V, Mennucci B, Petersson GA, Nakatsuji H, Caricato M, Li X, Hratchian HP, Izmaylov AF, Bloino J, Zheng G, Sonnenberg JL, Hada M, Ehara M, Toyota K, Fukuda R, Hasegawa J, Ishida M, Nakajima T, Honda Y, Kitao O, Nakai H, Vreven T, Montgomery JA, Jr., Peralta JE, Ogliaro F, Bearpark M, Heyd JJ, Brothers E, Kudin KN, Staroverov VN, Kobayashi R, Normand J, Raghavachari K, Rendell A, Burant JC, Iyengar SS, Tomasi J, Cossi M, Rega N, Millam JM, Klene M, Knox JE, Cross JB, Bakken V, Adamo C, Jaramillo J, Gomperts R, Stratmann RE, Yazyev O, Austin AJ, Cammi R, Pomelli C, Ochterski JW, Martin RL, Morokuma K, Zakrzewski VG, Voth GA, Salvador P, Dannenberg JJ, Dapprich S, Daniels AD, Farkas Ö, Foresman JB, Ortiz JV, Cioslowski J, Fox DJ (2009) Gaussian '09, Revision A.1. '09, Wallingford CT

Harris SA, McGuigan C, Andrei G, Snoeck R, De Clercq E, Balzarini J (2001) Synthesis and antiviral evaluation of phosphoramidate derivatives of (E)-5-(2-bromovinyl)-2′-deoxyuridine. Antivir Chem Chemother 12:293–300

Hehre W, Ohlinger S (2010) Spartan'10 Tutorial and user's guide. '10, Wavefunction Inc

Kašpárek F, Mollin J (1980) Solvolysis of diphenyl amidophosphates in aqueous alcoholic media. Collect Czech Chem Commun 52:1115–1130

Krajewska B (2009) Ureases I. Functional, catalytic and kinetic properties: a review. J Mol Catal B Enzym 59:9–21

Krishnan P, Sundaram S, Venkatasubramanian N (1985) Alkaline hydrolysis of arylesters of diphenylphosphorodiamidates—evidence consistent with an elimination—addition mechanism. Proc Indian Acad Sci Chem Sci 94:467–473

Li HQ, Xiao ZP, Yin L, Yan T, Lv PC, Zhu HL (2009) Amines and oximes derived from deoxybenzoins as *Helicobacter pylori* urease inhibitors. Eur J Med Chem 44:2246–2251

Lipinski CA, Lombardo F, Dominy BW, Feeney PJ (1997) Experimental and computational approaches to estimate solubility and permeability in drug discovery and development settings. Adv Drug Deliver Rev 23:3–25

Lipinski CA, Lombardo F, Dominy BW, Feeney PJ (2001) Experimental and computational approaches to estimate solubility and permeability in drug discovery and development settings. Adv Drug Deliv Rev 46:3–26

Maalej E, Chabchoub F, Samadi A, de Los Ríos C, Perona A, Morreale A, Marco-Contelles J (2011) Synthesis, biological assessment and molecular modeling of 14-aryl-10,11,12,14-tetrahydro-9*H*-benzo[5,6]chromeno[2,3-b]quinolin-13-amines. Bioorg Med Chem Lett 21:2384–2388

Mangal M, Sagar P, Singh H, Raghava GP, Agarwal SM (2013) NPACT: naturally occurring plant-based anti-cancer compound-activity-target database. Nucleic Acids Res 41:D1124–D1129

Mara C, Dempsey E, Bell A, Barlow JW (2011) Synthesis and evaluation of phosphoramidate and phosphorothioamidate analogues of amiprophos methyl as potential antimalarial agents. Bioorg Med Chem Lett 21:6180–6183

Marenich AV, Cramer CJ, Truhlar DG (2009) Universal solvation model based on solute electron density and on a continuum model of the solvent defined by the bulk dielectric constant and atomic surface tensions. J Phys Chem B 113:6378–6396

McGuigan C, Kelleher MR, Perrone P, Mulready S, Luoni G, Daverio F, Rajyaguru S, Pogam SL, Najera I, Martin JA, Klumpp K, Smith DB (2009) The application of phosphoramidate ProTide technology to the potent anti-HCV compound 4′-azidocytidine (R1479). Bioorg Med Chem Lett 19:4250–4254

Mehellou Y, Balzarini J, McGuigan C (2009) An investigation into the anti-HIV activity of 2′,3′-didehydro-2′,3′-dideoxyuridine (d4U) and 2′,3′-dideoxyuridine (ddU) phosphoramidate 'ProTide' derivatives. Org Biomol Chem 7:2548–2553

Oliveira FM, Barbosa LCA, Teixeira RR, Demuner AJ, Maltha CRA, Picanço MC, Silva GA, Paula VF (2012a) Synthesis and insecticidal activity of new phosphoramidates. J Pestic Sci 37:85–88

Oliveira FM, Barbosa LCA, Valente VMM, Demuner AJ, Maltha CRA, Oliveros-Bastidas AJ (2012b) Structure–activity relationship of pyridin-2(1*H*)-ones derivatives as urease inhibitors. J Pharm Res 5:5326–5333

Paula VF, Barbosa LCA, Teixeira RR, Picanco MC, Silva GA (2008) Synthesis and insecticidal activity of new 3-benzylfuran-2-yl *N*, *N*, *N*′, *N*′-tetraethyldiamidophosphate derivatives. Pest Manag Sci 64:863–872

Proudfoot JR (2002) Drugs, leads, and drug-likeness: an analysis of some recently launched drugs. Bioorg Med Chem Lett 12:1647–1650

Roberts BP, Miller BR 3rd, Roitberg AE, Merz KM Jr (2012) Wide-open flaps are key to urease activity. J Am Chem Soc 134:9934–9937

Roubinek F, Bedrník P, Cech M, Daněk J, Buděšínský Z (1980) Diphenylesters of amidophosphoric acids, their synthesis, determination of phosphorus and biological activity. Cesk Farm 29:90–94

Ruveda MA, Zerba EN, Podesta R, de Licastro SA (1975) Organophosphorus chemistry—V: thermal transformation of the cyclohexylammonium salt of *O*-aryl *N*-cyclohexyl phosphoramidic acids into sym-pyrophosphates. Tetrahedron 31:885–890

Tambunan US, Bramantya N, Parikesit AA (2011) In silico modification of suberoylanilide hydroxamic acid (SAHA) as potential inhibitor for class II histone deacetylase (HDAC). BMC Bioinf 12(Suppl 13):S23

Teixeira RR, Bressan GC, Pereira WL, Ferreira JG, Oliveira FM, Thomaz DC (2013) Synthesis and antiproliferative activity of C-3 functionalized isobenzofuran-1(3*H*)-ones. Molecules 18:1881–1896

Tetko IV (2005) Computing chemistry on the web. Drug Discov Today 10:1497–1500

Uckun FM, Venkatachalam TK, Erbeck D, Chen CL, Petkevich AS, Vassilev A (2005) Zidampidine, an aryl phosphate derivative of AZT: in vivo pharmacokinetics, metabolism, toxicity, and antiviral efficacy against hemorrhagic fever caused by Lassa virus. Bioorg Med Chem 13:3279–3288

Vassiliou S, Grabowiecka A, Kosikowska P, Yiotakis A, Kafarski P, Berlicki L (2008) Design, synthesis, and evaluation of novel organophosphorus inhibitors of bacterial ureases. J Med Chem 51:5736–5744

Veber DF, Johnson SR, Cheng HY, Smith BR, Ward KW, Kopple KD (2002) Molecular properties that influence the oral bioavailability of drug candidates. J Med Chem 45:2615–2623

Weatherburn MW (1967) Phenol-hypochlorite reaction for determination of ammonia. Anal Chem 39:971–974

Zhang G, Musgrave CB (2007) Comparison of DFT methods for molecular orbital eigenvalue calculations. J Phys Chem A 111:1554–1561